JOURNAL OF ENDOUROLOGY
Volume 27, Number 12, December 2013

Pp. 1487–1492
DOI: 10.1089/end.2013.0173

Effect of Magnesium on Calcium and Oxalate Ion Binding

Julie M. Riley, MD,[1] Hyunjin Kim, PhD,[2] Timothy D. Averch, MD,[1] and Hyung J. Kim, PhD[2]

Abstract

Background and Purpose: Magnesium (Mg^{2+}) has been shown to be a kidney stone inhibitor; however, the exact mechanism of its effect is unknown. Using theoretical models, the interactions of calcium and oxalate were examined in the presence of Mg^{2+}.

Methods: Molecular dynamics simulations were performed with NAMD and CHARMM27 force field. The interaction between calcium (Ca^{2+}) and oxalate (Ox^{2-}) ions was examined with and without magnesium. Concentrations of calcium and oxalate were 0.1 M and 0.03 M, respectively, and placed in a cubic box of length ~115 Angstrom. Na^{+} and Cl^{-} ions were inserted to meet system electroneutrality. Mg^{2+} was then placed into the box at physiologic concentrations and the interaction between calcium and oxalate was observed. In addition, the effect of citrate and pH were examined in regard to the effect of Mg^{2+} inhibition. Each system was allowed to run until a stable crystalline structure was formed.

Results: The presence of Mg^{2+} reduces the average size of the calcium oxalate and calcium phosphate aggregates. This effect is found to be Mg^{2+} concentration-dependent. It is also found that Mg^{2+} inhibition is synergistic with citrate and continues to be effective at acidic pH levels.

Conclusion: The presence of magnesium ions tends to destabilize calcium oxalate ion pairs and reduce the size of their aggregates. Mg^{2+} inhibitory effect is synergistic with citrate and remains effective in acidic environments. Further studies are needed to see if this can be applied to *in vivo* models as well as extending this to other stone inhibitors and promoters.

Introduction

The role of magnesium (Mg^{2+}) as an inhibitor for calcium oxalate (CaOx) stone formation is controversial because of conflicting results in recent clinical trials.[1–4] Using molecular dynamics and theoretical chemistry modeling, we examine the role of the Mg^{2+} ion in calcium and oxalate binding.

Methods

Using the NAMD program, molecular dynamics (MD) simulations were performed to evaluate the role of Mg^{2+} in calcium and oxalate binding.[5] NAMD is a molecular dynamics code used in the examination of large systems, including biologic systems. Using CHARMM potential functions, NAMD describes individual particles at a molecular level with force field specifications.[5] All ions studied used the CHARMM27 force field.[6,7] Force field parameters determined by Yesselman and associates[8] via MATCH were used for Ox^{2-} and citrate (Cit^{3-}), while those for phosphate (PO_4^{3-}) and dihydrogen phosphate ($H_2PO_4^{-}$) were determined using CHARMM general force field (CGenFF)[9] in the CHARMM program. The standard TIP3P potential model was used for water.[10] The short-range repulsion and dispersion (Lennard-Jones interactions) and long-range Coulombic forces were evaluated and the Newton equation of motion was integrated to propagate the dynamics of the system.

Table 1 outlines the components of each system design. To avoid any confusion, we mention that size of systems 1 and 2 is small; specifically, they are 15 times smaller than systems 4 to 10. We used systems 1 and 2 to simply evaluate the interaction of Ca^{2+} and Ox^{2-} in the absence and presence of Mg^{2+} via the free energy calculations. System 1 consists of one pair of Ca^{2+} and Ox^{2-} and 3330 water molecules. In addition, 10 pairs (~0.16 M) of Na^{+} and Cl^{-} ions were added, so that its overall salt concentration is close to the physiologic condition. Compared with system 1, one Mg^{2+} and two additional Cl^{-} ions were added to system 2. The latter is to meet the system electroneutrality. The levels of the ions were supraphysiologic to observe any effect within the constraints of the computing power. After equilibration, we computed free energies of systems 1 and 2, using the metadynamics algorithm.[11] Two coordinates, $\rho = \sqrt{x^2 + y^2}$ and z, of the cylindrical coordinate system were used to describe the position of the calcium ion with respect to oxalate (Fig. 1). For each system, the simulation was performed for 400 ns with a time step of 2 fs, and free

[1]Department of Urology, University of Pittsburgh Medical Center, Pittsburgh, Pennsylvania.
[2]Department of Chemistry, Carnegie Mellon University, Pittsburgh, Pennsylvania.

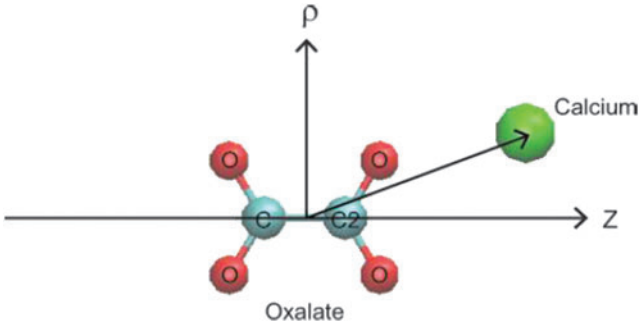

FIG. 1. Coordinates of calcium and oxalate: ρ and z are defined as the displacement of Ca^{2+} from the Ox^{2-} center-of-mass along the carbon–carbon bond in Ox^{2-} and its perpendicular directions, respectively. Ca^{2+} ion is represented in the green sphere and O and C atoms of Ox^{2-} are in red and light blue, respectively. Visual Molecular Ddynamics[18] is used for display.

energies were obtained by averaging over the azimuthal angle coordinate θ.[8]

The free energy results for Ca^{2+} and Ox^{2-}, in particular, local minima, provide information on the Ca^{2+}-Ox^{2-} binding affinity and structures and their variations with the presence of other ions. Deeper energy minima indicate the formation of a more stable calcium-oxalate ion pair, thereby suggesting that calcium and oxalate ions are more likely to aggregate. Within our model, we are able to determine both the value and location of the free energy minima. We should note, however, that the effect of many urinary ionic species as well as that of heterogeneous biologic environments is ignored in the free energy calculations.

With systems 3 to 10, we investigated aggregation dynamics of CaOx in the absence and presence of various urine ions that are either known stone promoters or inhibitors of low weight.[12–17] System 3 was composed of 22 pairs of Ca^{2+} and Ox^{2-} ions, 30 pairs of Na^+ and Cl^- ions, and 10000 water molecules. For systems 4 to 10, 90 Ca^{2+} and 30 Ox^{2-} were immersed in water consisting of 50,000 water molecules. The salt concentration was adjusted to satisfy the system electroneutrality. Systems 4, 5, and 6 that model a pH neutral/basic environment differ in their magnesium concentration; ie, 0, 83, and 150 mM, respectively (Table 1). For systems 7 and 8, citrate was inserted to evaluate its effect on aggregates. Systems 9 and 10 were generated from systems 4 and 6 by replacing their PO_4^{3-} ions with $H_2PO_4^-$ to model an acidic urine environment. This allows us to study how pH influences Ca^{2+}-Ox^{2-} aggregation. 100 ns, 80 ns and 40 ns MD simulations were performed for system 3, systems 4 to 8, and systems 9 and 10, respectively.

Table 1. Ionic Concentrations in Each System

System	*Concentrations in mM*						
	Ca^{2+}	Ox^{2-}	Mg^{2+}	Cit^{3-}	$H_2PO_4^-$	NH_4^+	PO_4^{3-}
1	16	16	0	0	0	0	0
2	16	16	16	0	0	0	0
3	120	120	0	0	0	0	0
4	100	33	0	0	0	150	150
5	100	33	83	0	0	150	150
6	100	33	150	0	0	150	150
7	100	33	0	33	0	150	150
8	100	33	150	33	0	150	150
9	100	33	0	0	150	150	0
10	100	33	150	0	150	150	0

Results

In system 3, a large aggregate was formed around 30 ns. This structure continued to grow and become stabilized through association and dissociation of Ca^{2+} and Ox^{2-} ions along its edges. After ~50 ns, a stable structure was formed, and no significant dissociation or association along its edges was observed in the remainder of the simulation. The structure of the aggregate at 100 ns is shown in Figure 2. Its analysis reveals three important configurations for the binding pair. Specifically, Ca^{2+} ions bind to the O-C-O (b1) or the O-C-C-O (b2) pockets of the Ox^{2-} anion. Oxygen atoms (b3) of oxalate can also function as a third cation binding site to form an ion pair with Ca^{2+}.[8]

The free energy of a Ca^{2+} and Ox^{2-} complex determined as a function of ρ and z shows that its global minimum is located at the b2 position (viz., $\rho \sim 2.8$Å and z = 0 Å) of oxalate (Fig. 3A). This means that b2 is the strongest Ca^{2+} binding site of Ox^{2-} when no promoter and/or inhibitor ions are present in the system. Local minima at $\rho = 0$Å and z = ~ ±3 Å and at

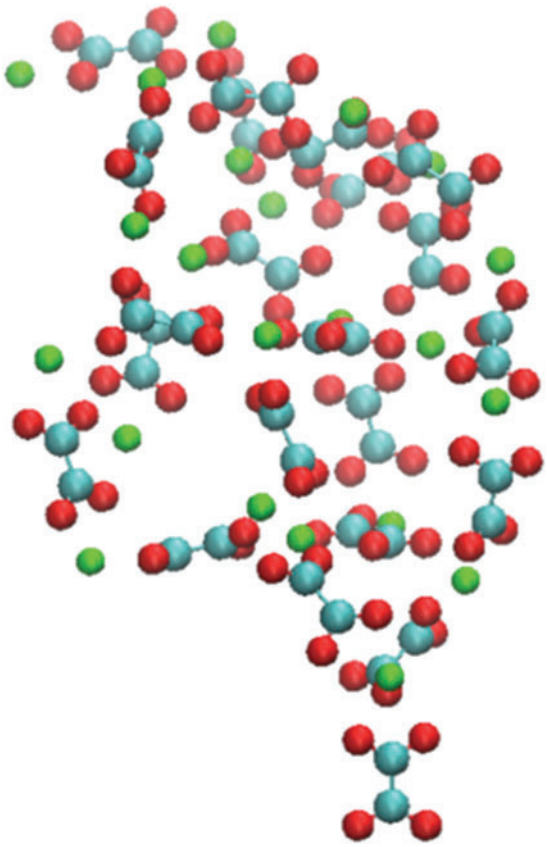

FIG. 2. Structure of the calcium-oxalate aggregate obtained from the 100 ns MD simulation of system 3. Ca^{2+} is represented in the green sphere and oxygen and carbon atoms in Ox^{2-} are in red and blue spheres, respectively. Visual Molecular Dynamics was used to display the structure.[18]

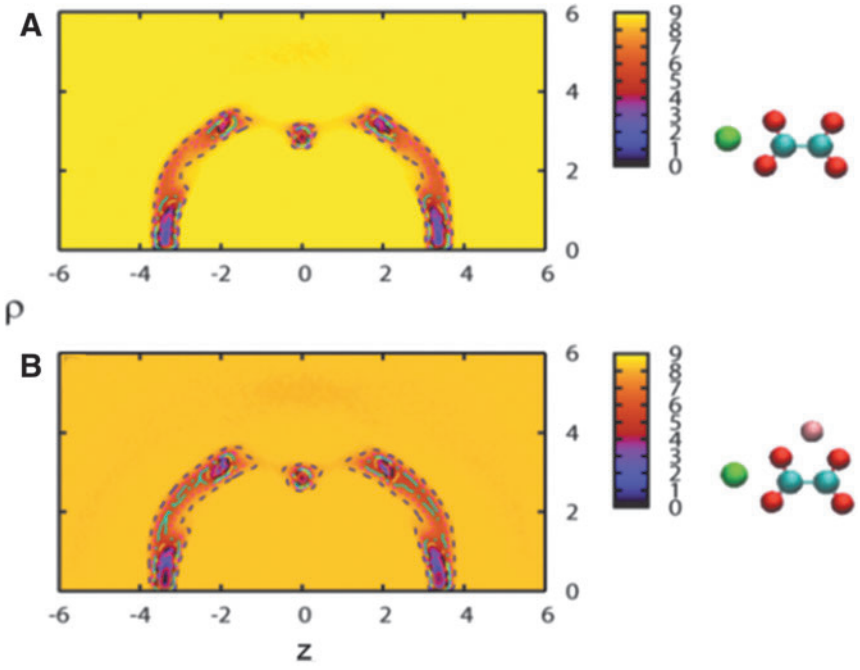

FIG. 3. Two-dimensional free energy map for the Ca^{2+}-Ox^{2-} complex in an aqueous solution of NaCl: **(A)** System 1 and **(B)** system 2. The free energy is measured in kcal/mol and increases as its color changes from dark purple to light yellow. In each case, pre-equilibrated structure of ions used as an initial configuration in metadynamics simulations is shown next to the contour map. Mg^{2+} ion is represented in the pink sphere. (Units for ρ and z: Å)

$\rho \sim 3.2$Å and $z = \sim \pm 2$ Å represent the second and third most stable binding sites, corresponding to b1 and b3, respectively.

Compared with system 1, system 2 shows a slight decrease in the Ca^{2+} and Ox^{2-} binding affinity because of the presence of Mg^{2+} (Fig. 3B). Mg^{2+} initially placed near the b2 site binds to the site during the equilibration (Fig. 3B). In the ensuing 400 ns simulation, it tends to move from one binding site to another and hinder the binding of Ca^{2+}. Because Mg^{2+} is smaller, it can "fit" into the binding sites of Ox^{2-} better than Ca^{2+}. This can prevent the binding of Ca^{2+} and Ox^{2-} at least

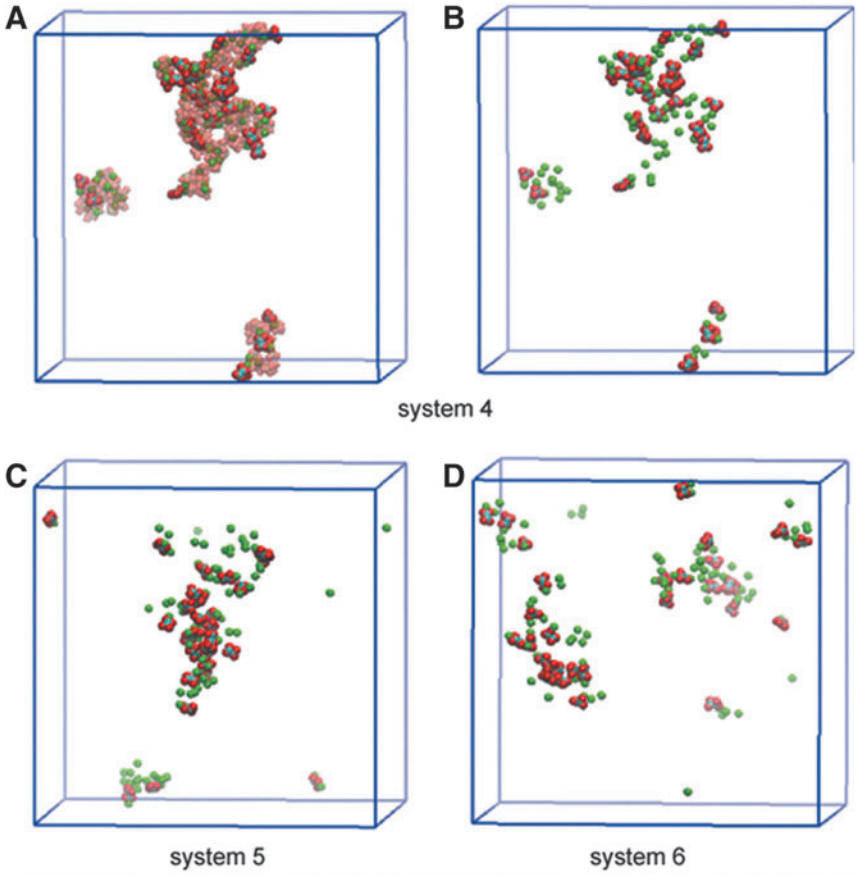

FIG. 4. Comparison of Ca^{2+} and Ox^{2-} aggregate in relation to Mg^{2+} concentration. In **B–D,** only Ca^{2+} and Ox^{2-} ions are displayed to clearly expose the difference among systems 4–6, while **A** also displays PO_4^{3-} ions (transparent) for system 4.[18] System 6, which is the highest in Mg^{2+} concentration among the three systems shown here, yields the smallest calcium phosphate/calcium oxalate aggregates. Although not shown in D, Mg^{2+} ions are located near Ox^{2-} ions instead of directly binding to them.

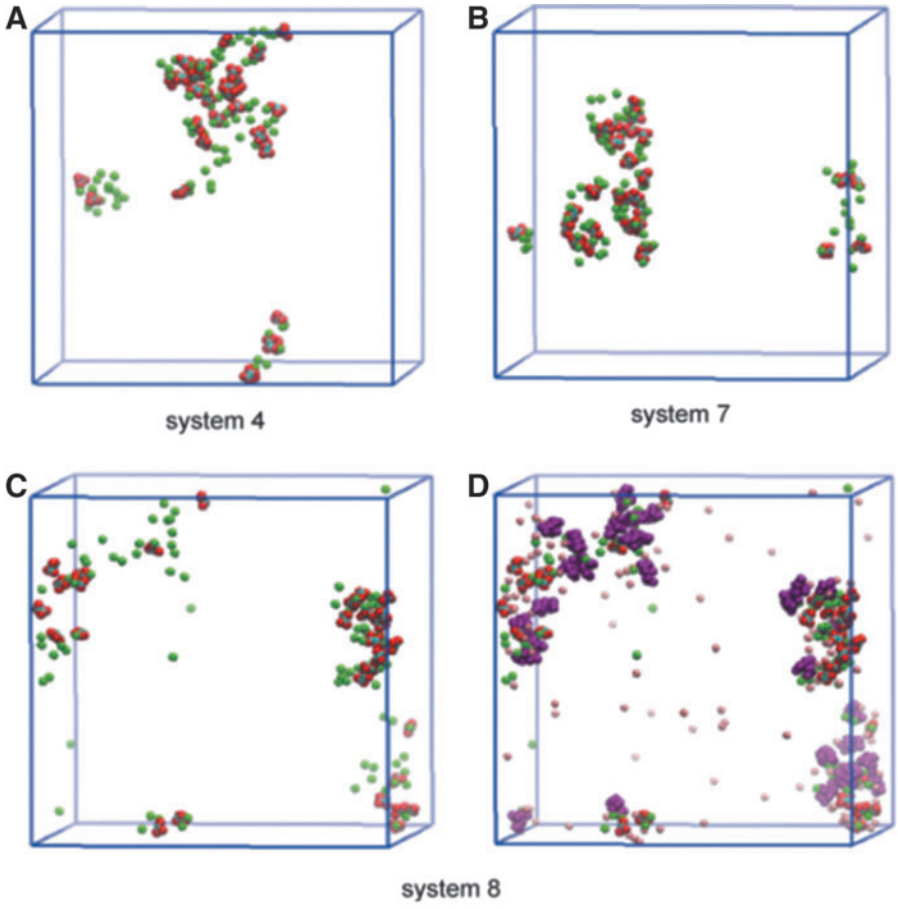

FIG. 5. Effect of Mg^{2+} and Cit^{3-}. In **A–C**, only Ca^{2+} and Ox^{2-} ions are shown, while Mg^{2+} (pink) and Cit^{3-} (purple) are also displayed in **D.**[18] There is synergy of the inhibitory effect on Ca^{2+} and Ox^{2-} aggregation.

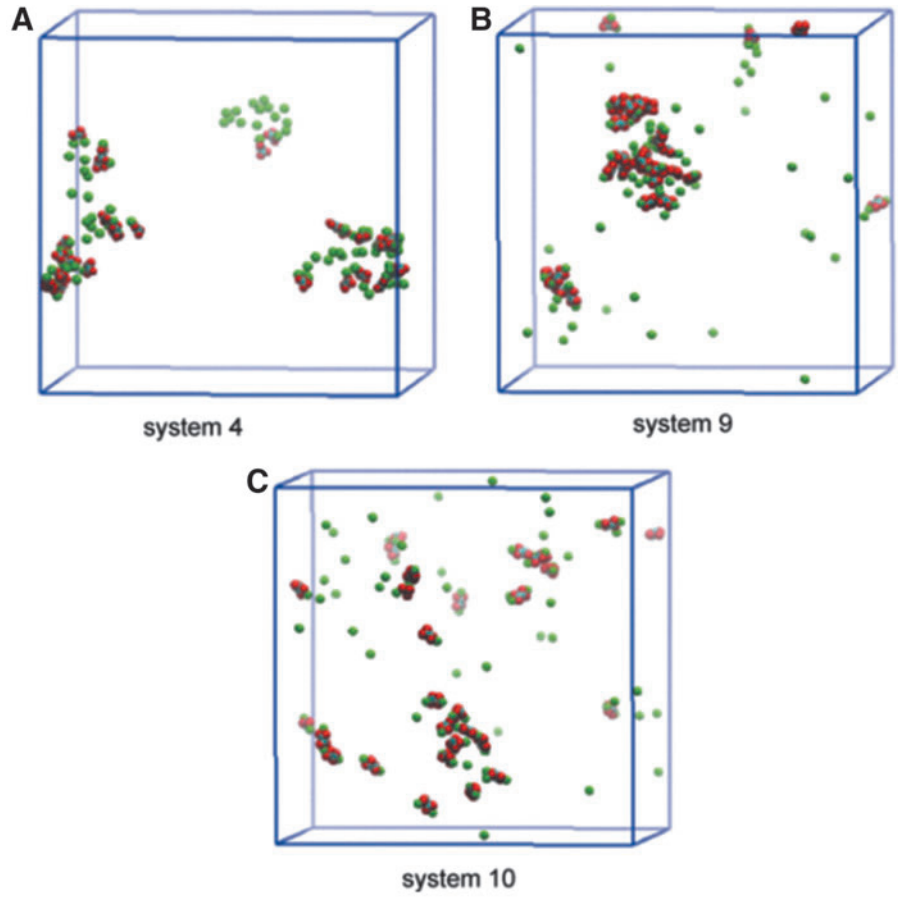

FIG. 6. Effect of pH. All snapshots were taken at 40 ns of the simulations. The aggregates of system 4 in **A** have mainly the CaP character while they are primarily CaOx aggregates in a more acidic environment in **B** and **C.** Aggregate size difference between the latter two indicates that Mg^{2+} continues to exert its inhibitory effect in the weakly acidic urine environment.

at the Mg^{2+} occupied sites and, as a result, slow down the aggregation of Ca^{2+} and Ox^{2-}. This paints the picture that Mg^{2+} and Ca^{2+} would compete directly for binding sites on Ox^{2-}. The presence of shallow secondary free energy minima for Mg^{2+}- Ox^{2-} complexation, however, complicates this picture. As Mg^{2+} ions approach Ox^{2-} from a distance, they can be trapped in these shallow wells. This could decelerate the binding of magnesium and considerably lower its ability to compete with Ca^{2+} to occupy the binding sites of Ox^{2-}. To obtain further insight into this issue and the roles of Mg^{2+}, we studied the formation of aggregates involving calcium explicitly via MD using systems 4 to 10 (Table 1).

Figure 4 shows the aggregate structures obtained for systems 4 to 6. We notice that Ca^{2+} form aggregates mainly with PO_4^{3-} because of the strong Coulombic interaction of the latter. As a result, aggregates are primarily made up of Ca^{2+}-PO_4^{3-} (CaP) binding structure mixed with some CaOx structure (Fig. 4A). The most salient aspect of Figure 4 is that the size of CaOx/CaP aggregates generally decreases as the Mg^{2+} concentration is raised. As shown in Figure 4B–D, however, the difference in the aggregate size between the 0 mM (system 4) to 83 mM (system 5) cases is not significant, compared with the difference of systems 5 (83 mM) and 6 (150 mM). These results indicate that Mg^{2+} has an inhibitory effect on CaOx/CaP aggregation, but this effect is magnesium concentration-dependent.

Systems 7 and 8 evaluated the role of citrate in inhibition in the absence and presence of magnesium. Comparison of the results in Figure 5A and B suggests that citrate alone does not have a significant influence on the size of CaP aggregates. We speculate that citrate does not compete with PO_4^{3-} because PO_4^{3-} presents in higher concentration than citrate in the system, although they have the same valency. Because the aggregation is mainly effected via PO_4^{3-} in the present case, citrate therefore tends to show little effect on CaP. The addition of citrate alone, however, can have an inhibitory effect on the formation of CaOx aggregates by directly competing with Ox^{2-} for binding Ca^{2+}, which is consistent with our previous free energy result. The role of citrate more clearly appears when both citrate and Mg^{2+} are present (Figs. 5C and D). Interestingly, when citrate was added with Mg^{2+}, a synergistic effect was seen, as manifested by the small size of CaOx/CaP aggregates in system 8 (Fig. 5C).

Finally, the effect of urinary pH and Mg^{2+} was explored in systems 9 and 10 (Figs. 6B and C). $H_2PO_4^-$ was used, which would be seen in a weakly acidic urine, as opposed to PO_4^{3-}, which would be seen in the more pH neutral and/or basic environment. In this sense, the replacement of PO_4^{3-} by $H_2PO_4^-$ effectively represents lowering of pH. This results in the formation of mainly CaOx aggregates, because Ca^{2+} ions are no longer intercepted by trivalent phosphate and thus become more available to interact with Ox^{2-} ions. This demonstrates the expected results of increase in CaOx aggregates in acidic urine. When Mg^{2+} was added to the system, the inhibitory effect as previously shown was maintained within this acidic milieu (Fig. 6C). We should note that Mg^{2+} ions on average do not actively participate in aggregation; ie, in most cases, they do not bind tightly to Ox^{2-}. This seems to support our earlier view that Mg^{2+} screens the interactions of Ca^{2+} with Ox^{2-} rather than directly competing with Ca^{2+} for the binding sites on Ox^{2-}.

Discussion

Mg^{2+} has been poorly understood within the literature. It is known to be an inhibitor, but the clinical application remains elusive.[1–4] Using MD, theoretical chemistry has allowed us to examine the molecular mechanism of the interaction of Mg^{2+} with Ca^{2+} and Ox^{2-} along with other known promoters and inhibitors. This will ultimately allow for a backbone to begin clinical applications of Mg^{2+} in stone formation.

While theoretical modeling has been used in stone disease, there has not been a previously described application to Mg^{2+} particularly with the obtained calcium oxalate aggregates.

While MD is able to provide information regarding ionic interaction, there are limitations in its use. Primarily, the biggest limitation to date is the inability to run computer experiments at physiologic concentrations. While we have been able to obtain the overall ionic concentrations close to urinary conditions, the concentrations of key ions, such as calcium and oxalate, still remain significantly higher than those seen in normal human urine. Because of the time constraints of the computer simulation, these concentrations were chosen to be significantly high. In addition, these are highly controlled experiments and certainly do not contain all of the species present within human urine. As the technology advances, the experiments have included more constituents but still remain far from physiologic. Finally, this remains theoretical and the application to *in vivo* studies is unknown.

Further studies are warranted at this time to examine stone formation at physiologic concentrations. In addition, we would like to study Mg^{2+} inhibition within human models.

Conclusion

The ion pair interaction of Ca^{2+} and Ox^{2-} ions is weakened in the presence of magnesium, indicating a shortened contact time. The effect of Mg^{2+} appears to be influenced by its density as well as its positions with respect to Ox^{2-}. Mg^{2+} inhibitory effect is synergistic with citrate and remains effective in acidic environments. Further studies are needed to see if this can be applied to *in vivo* models as well as extending this to other stone inhibitors and promoters.

Acknowledgment

We are grateful to the National Institute for Computational Sciences (NICS) for the supercomputing time grant, Kraken TG-MCB100064.

Disclosure Statement

No competing financial interests exist.

References

1. Guerra A, Meschi T, Allegri F, et al. Concentrated urine and diluted urine: The effects of citrate and magnesium on the crystallization of calcium oxalate induced *in vitro* by an oxalate load. Urol Res 2006;34:359–364.
2. Jaipakdee S, Prasongwatana V, Premgamone A, et al. The effects of potassium and magnesium supplementations on urinary risk factors of renal stone patients. J Med Assoc Thai 2004;87:255–263.
3. Kato, Y, Yamaguchi S, Yachiku S, et al. Changes in urinary parameters after oral administration of potassium-sodium

citrate and magnesium oxide to prevent urolithiasis. Urology 2004;63:7–12.
4. Schwille PO, Schmiedl A, Herrmann U, et al. Magnesium, citrate, magnesium citrate and magnesium-alkali citrate as modulators of calcium oxalate crystallization in urine: Observations in patients with recurrent idiopathic calcium urolithiasis. Urol Res 1999;27:117–126.
5. Phillips JC, Bruan R, Wang W, et al. Scalable molecular dynamics with NAMD. J Comp Chem 2005;26:1781–1802.
6. Brooks BR, Bruccoleri RE, Olafson BD, et al. CHARMM: A program for macromolecular energy, minimization, and dynamics calculations. J Comp Chem 1983;4:187–217.
7. Mackerell AD, Brooks B, Brooks CL III, et al. CHARMM: The energy function and its parameterization with an overview of the profram. In: P. v. R. Schleyer et al., eds. The Encyclopedia of Computational Chemistry. Berne, Switzerland: John Wiley and Sons, 1998, 1, pp 271–277.
8. Yesselman JD, Price DJ, Knight JL, Brooks CL III. MATCH: An atom-typing toolset for molecular mechanics force fields. J Comp Chem 2012;33:189–202.
9. Vanommeslaeghe K, Hatcher E, Acharya C, et al. CHARMM General Force Field (CGenFF): A force field for drug-like molecules compatible with the CHARMM all-atom additive biological force fields. J Comput Chem 2010;31:671–690.
10. Jorgensen WL, Chandrasekhar J, Madura JD, et al. Comparison of simple potential functions for simulating liquid water. J Chem Phys 1983;79:926–935.
11. Laio A, Parrinello M. Escaping free-energy minima. Proc Natl Acad Sci U S A 2002;99:12562–12566.
12. Lemann J, Litzow JR, Lennon EJ. Studies of the mechanism by which chronic metabolic acidosis augments urinary calcium excretion in man. J Clin Invest 1967;46:1318–1328.
13. Barcelo P, Wuhl O, Servitge E, et al. Randomized double-blind study of potassium citrate in idiopathic hypocitraturic calcium nephrolithiasis. J Urol 1993;150:1761–1764.
14. Fuselier HA, Moore K, Lindberg J, et al. Agglomeration inhibition reflected stone-forming activity during long term potassium citrate therapy in calcium stone formers. Urology 1998;52:988–994.
15. Grover PK, Marshall VR, Ryall RL. Dissolved urate salts out calcium oxalate in undiluted human urine *in vitro*: Implications for calcium oxalate stone genesis. Chem Biol 2003; 10:271–278.
16. Khan SR, Shevock PN, Hackett RL. Magnesium oxide administration and prevention of calcium oxalate nephrolithiasis. J Urol 1993;149:412–416.
17. Siener R, Jahnen A, Hesse A. Bioavailability of magnesium from different pharmaceutical formulations. Urol Res 2011; 39:123–127.
18. Humphrey W, Dalke A, Schulten K. VMD: Visual molecular dynamics. J Mol Graph 1996;14:33–38.

Address correspondence to:
Julie M. Riley, MD
Department of Urology
University of Pittsburgh Medical Center
3471 Fifth Ave., Suite 700
Pittsburgh, PA 15213

E-mail: rileyj@salud.unm.edu

Abbreviations Used

Ca^{2+} = calcium
CaOx = calcium oxalate
CaP = calcium phosphate
Cl^- = chloride
Cit^{3-} = citrate
fs = femtosecond
$H_2PO_4^-$ = dihydrogen phosphate
MD = molecular dynamics
Mg^{2+} = magnesium
Na^+ = sodium
ns = nanosecond
Ox^{2-} = oxalate
PO_4^{3-} = phosphate